IMMUNOLOGY

PD-1 and ICOS are coexpressed in T follicular helper cells but define three stages of maturation of T follicular regulatory cells

Filipa Ribeiro[1,2], Diogo Antunes[1,2], Ana R. Pires[1], José Rino[1], Beatriz Filipe[1], Kátia Jesus[1], Ricardo Correia[1], Válter R. Fonseca[1,2], Saumya Kumar[1,3]†, Luis Graca[1,2]*†

Humoral responses to infection or vaccination require T cell–B cell interactions. T follicular helper (T_{FH}) cells drive germinal center (GC) responses by providing help to B cells, whereas T follicular regulatory (T_{FR}) cells regulate them. Both mature GC–located T_{FH} and T_{FR} cells are widely characterized by the expression of ICOS and PD-1. However, although human T_{FR} cells share many phenotypic characteristics with T_{FH} cells, we found that ICOS and PD-1 are up-regulated differently in each. Although T_{FH} cells express these proteins synchronously during maturation, they define three maturation stages in T_{FR} cells. T_{FR} cells in an intermediate maturation stage express ICOS, and it is only at the last stage of differentiation that both molecules are expressed at high levels. Although most T_{FR} cells within the B cell follicle are PD-1^-, the T_{FR} within the GC are ICOS$^+$PD-1^+. These results show that T_{FH} and T_{FR} cells within human lymphoid tissue follow distinct maturation stages.

INTRODUCTION

The findings of T follicular helper (T_{FH}) and T follicular regulatory (T_{FR}) cells controlling germinal center (GC) reactions in mice prompted the study of T follicular subsets in humans. Whereas T_{FH} cells provide help to B cells (*1*), T_{FR} cells suppress the GC response and limit the overall expansion of antigen-specific B cell clones (*2*–*4*). The absence of T_{FR} cells is related to the emergence of autoimmunity in mice (*5*, *6*). Further studies to better understand the definition and function of human T_{FR} cells are critical, which may help in understanding how GC reactions affect dysregulated immune responses, such as autoimmunity and open avenues for its modulation in the future.

The definition of T_{FR} cells has been controversial, given the diversity of T_{FR} populations with distinct origin (*7*–*11*), and the fact that the T_{FR} cell biology has not been described with the same detail as T_{FH} cells. Because of the absence of lineage-defining markers exclusive to T_{FR} cells, the phenotype and differentiation of T_{FR} cells have been frequently studied by extrapolating T_{FH} cell data. CXCR5 has been a key defining follicular marker for T_{FH} and T_{FR} cells as its expression correlates with the follicular location in both cases (*12*, *13*). Moreover, anatomical positioning of T_{FH} cells within GC is also governed by the signaling of ICOS (*14*, *15*), which supports CXCR5$^+$ T cell migration toward the follicle and PD-1 by promoting the retention of T_{FH} cells in the GC (*16*). Therefore, these two receptors have been widely used, together with CXCR5, to define GC T_{FH} cells in both humans and mice. It has been assumed that T_{FR} cells follow a differentiation process similar to that of T_{FH} cells, and therefore, the same markers have been used to identify both cell subsets (*17*). Besides the molecules associated with regulatory T (T_{reg}) cells (such as FOXP3 and/or CD25), a combination of two proteins is commonly used to identify lymphoid tissue T_{FR} cells: CXCR5 with either ICOS or PD-1, which are often used interchangeably.

Nevertheless, the follicle positioning of T_{FR} cells in human lymph nodes was shown to be determined by CXCR5 expression but not by PD-1 expression as for T_{FH} cells (*13*). Thus, we hypothesized that PD-1 and ICOS expression does not follow the same profile in T_{FH} and T_{FR} cells, and consequently, they cannot be used interchangeably to define T_{FR} cells as they are for T_{FH} cells. This was successfully demonstrated in the current study.

A major constraint in the field of T_{FR} cells is the difficulty in isolating human T_{FR} cells from lymphoid tissues with a high degree of purity due to the lack of surface markers that discriminate this cell population from others. One of the major challenges of studying human T_{FR} cells is the absence of known cell surface markers that can uniquely define them, without being also present in T_{FH}, CD25$^+$ interleukin-10 (IL-10)–producing T follicular cells (IL-10 TF), or T_{reg} cells. A better understanding of ICOS and PD-1 expression dynamics in human lymphoid tissue T_{FR} cells allowed us to explore innovative strategies to isolate this cell population for potential downstream analysis.

RESULTS

ICOS and PD-1 are expressed differently in T_{FH} and T_{FR} cells within human secondary lymphoid tissue

We analyzed 50 tonsil samples by flow cytometry and applied a permissive strategy, based only on the expression of FOXP3 and CXCR5, to define T_{FH} (CD4$^+$FOXP3$^-$CXCR5$^+$CD25$^-$) and T_{FR} cells (CD4$^+$FOXP3$^+$CXCR5$^+$). Using this strategy, the IL-10 TF cells (CD4$^+$FOXP3$^-$CXCR5$^+$CD25$^+$) were not included in the study (*18*, *19*).

Within the cell subsets defined as T_{FH} and T_{FR}, we explored the presence of the activation markers ICOS and PD-1 known to be characteristic of the most mature cells within the GC (*17*) (Fig. 1A). Tonsil T_{FH} and T_{FR} cells have a clearly different PD-1/ICOS profile: Whereas the expression of ICOS and PD-1 correlates almost perfectly in T_{FH} cells, appearing to be interchangeable, this is not the case for T_{FR} cells (Fig. 1B). In the latter, the correlation between the ICOS and PD-1 is weak, indicating that these proteins cannot be used interchangeably to identify T_{FR} cells as they are for T_{FH} cells. We therefore hypothesize that, although T_{FH} cells mature from

[1]Gulbenkian Institute for Molecular Medicine, Lisboa, Portugal. [2]Faculdade de Medicina, Universidade de Lisboa, Lisboa, Portugal. [3]Centre for Individualised Infection Medicine (CiiM), a joint venture between the Helmholtz Centre for Infection Research (HZI) and Hannover Medical School (MHH), Hannover, Germany.
*Corresponding author. Email: lgraca@medicina.ulisboa.pt
†These authors contributed equally to this work.

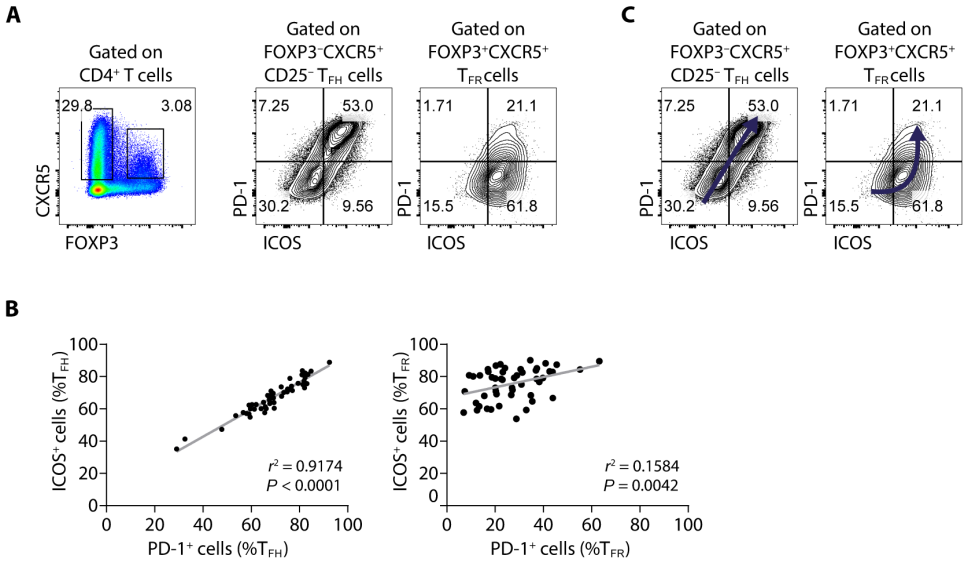

Fig. 1. ICOS and PD-1 are expressed differently in tissue T_{FH} and T_{FR} cells in humans. (**A**) Presence of ICOS and PD-1 on the surface of T_{FH} ($CD4^+FOXP3^-CXCR5^+CD25^-$) and T_{FR} cells ($CD4^+FOXP3^+CXCR5^+$) in human tonsils. Density plot showing the gate used to define T_{FH} cells ($CXCR5^+FOXP3^-$) and T_{FR} cells ($CXCR5^+FOXP3^+$) and two representative contour plots showing the distribution of PD-1 and ICOS among the T_{FH} and T_{FR} gates. (**B**) Relationship of the percentage of $ICOS^+$ and $PD\text{-}1^+$ cells within T_{FH} (left) and T_{FR} cells (right) in tonsil ($n = 50$; linear regression). (**C**) Diagram with a model for the trajectory of T_{FH} and T_{FR} maturation defined by PD-1 and ICOS, where T_{FH} cells transit from a double-negative to a double-positive stage (left), whereas T_{FR} cells have three stages: double-negative, $ICOS^+PD\text{-}1^-$, and lastly double-positive.

$ICOS^-PD\text{-}1^-$ toward an $ICOS^+PD\text{-}1^+$ phenotype, acquiring the two receptors simultaneously and at a similar rate, the maturation of T_{FR} cells from an $ICOS^-PD\text{-}1^-$ to the most mature $ICOS^+PD\text{-}1^+$ stage occurs in two stages. The first stage involves the up-regulation of ICOS, followed by a subsequent increase in the production of PD-1 (Fig. 1C).

Human T_{FH} and T_{FR} cells follow different maturation axes

To test our hypothesis, we analyzed the expression of the transcription factor BCL6, known to be up-regulated by the mature GC cells (*20*), and CD45RO, also known to be more expressed in mature T cells (*21*). It is noteworthy that CD45RO is a marker of activated T cells and, given that T follicular cells are already in an activated state, it is reasonable to anticipate some production of this protein even in less mature follicular cells.

In T_{FH} cells, two major populations were considered: $ICOS^-PD\text{-}1^-$ and $ICOS^+PD\text{-}1^+$ cells (Fig. 2A and fig. S1). The $ICOS^+PD\text{-}1^+$ population represents the most mature T_{FH} cells, characterized by a predominant coexpression of BCL6 and CD45RO, that are present at high concentrations (as inferred from the fluorescence intensity) (Fig. 2, B and C). By extracting the fluorescence intensity of seven markers used in the flow cytometry analysis and using principal components analysis (PCA), we were able to explore the relationship between all markers at the same time. The PCA of T_{FH} cells shows that PC1 is the component that contributes the most to the variance (69.70%) and is therefore sufficient to explain the linear maturation of T_{FH} cells (Fig. 2, D and E). PD-1 and ICOS are the proteins that contribute the most to PC1 and with a similar influence (0.97 and 0.92, respectively) (Fig. 2E). PC2 is not shown as it mainly segregates $CD45RO^+$ and $CD45RO^-$ T_{FH} populations (fig. S2).

Next, we analyzed the T_{FR} population using the same approach. T_{FR} cells can be subdivided into three populations according to the PD-1/ICOS axis: $ICOS^-PD\text{-}1^-$, $ICOS^+PD\text{-}1^-$, and $ICOS^+PD\text{-}1^+$ cells (Fig. 3A and fig. S1). Similar to T_{FH} cells, the $ICOS^+PD\text{-}1^+$ T_{FR} population contains the most mature cells as BCL6 and CD45RO are more abundant compared to the other subpopulations (Fig. 3, B and C). Within this population, $BCL6^+$ cells exhibit the highest CXCR5 expression, further reinforcing their advanced maturation within the GC (fig. S3). In addition, the expression of CD25 (IL-2 receptor α chain) was also assessed in the different compartments. It is established that T_{FR} cells lose CD25 in the last stages of their differentiation as they become mature GC T_{FR} cells (*19*, *22*–*24*). The $ICOS^+PD\text{-}1^+$ T_{FR} population comprises a greater frequency of $CD25^-$ cells, also supporting that this T_{FR} compartment contains the most mature T_{FR} cells (Fig. 3, B and C). According to the production of BCL6, CD45RO, and CD25, T_{FR} cells seem to display ICOS on their surface before up-regulating PD-1 and reaching a fully mature state. However, we observed a substantial number of $CD25^-$ cells within the $ICOS^-PD\text{-}1^-$ T_{FR} compartment that was not expected, given their overall less mature phenotype (namely, regarding PD-1 and ICOS expression) (Fig. 3, B and C, and fig. S4). This could be explained by the possible existence of some $CD25^-$ T_{reg} cells even outside the GC (*25*, *26*).

Unlike what we observed for T_{FH} cells, the variance of the T_{FR} cell data is not explained by only one principal component, but with both PC1 and PC2 having a similar impact on the variance (38.97 and 28.84%, respectively) (Fig. 3, D and E). The correlation matrix of the expression of the different markers in T_{FR} cells shows that, whereas PC-1 explains the up-regulation of PD-1 and BCL6 and the down-regulation of CD25, PC2 describes the up-regulation of ICOS and CD45RO (Fig. 3E). The up-regulation of CXCR5 is described by both PC1 and PC2 (Fig. 3E). Therefore, whereas T_{FH} maturation is linear and explained by only one axis, the T_{FR} cell maturation is explained by two different axes, with one of the axes associated with PD-1 and the other with ICOS. Consequently, ICOS and PD-1 cannot be used interchangeably to identify T_{FR} cells as three populations are defined based on the expression of these receptors.

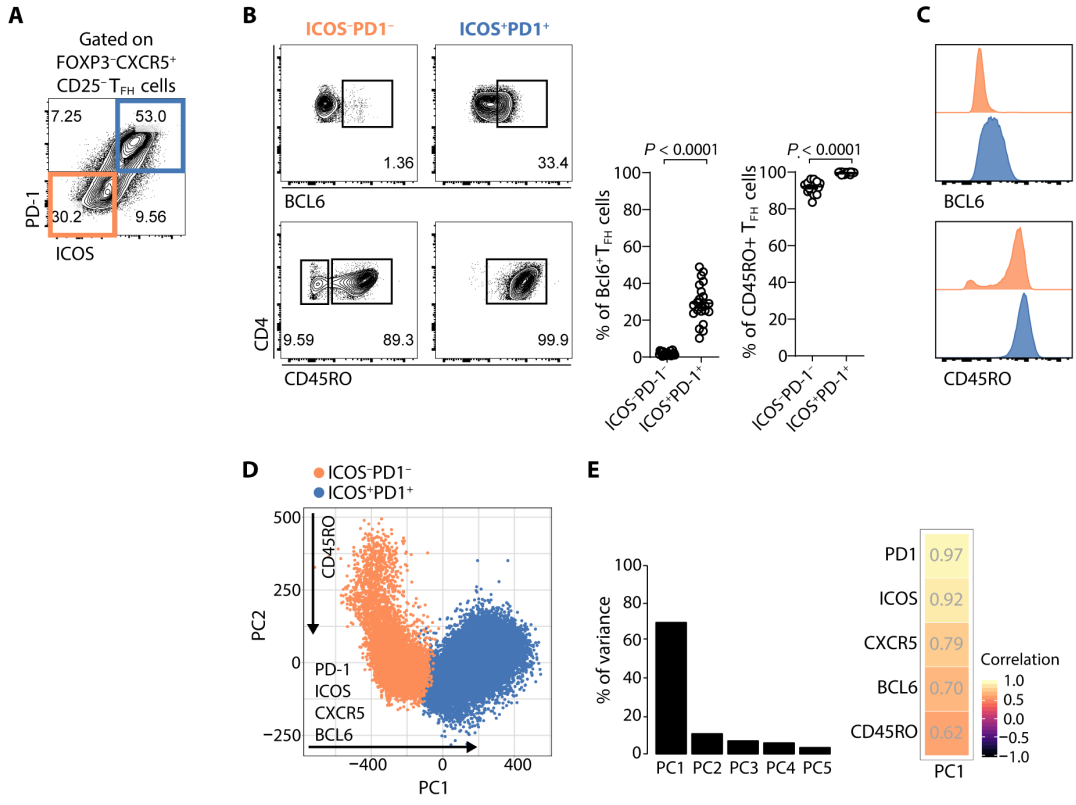

Fig. 2. ICOS and PD-1 expression increase in a coordinated way throughout the maturation of human T_{FH} cells. (**A**) Identification of the ICOS$^-$PD-1$^-$ (orange) and ICOS$^+$PD-1$^+$ (blue) subsets within tonsil CD4$^+$FOXP3$^-$CXCR5$^+$CD25$^-$ T_{FH} cells by flow cytometry. (**B**) Frequency of cells positive for BCL6 and CD45RO within the ICOS$^-$PD-1$^-$ and ICOS$^+$PD-1$^+$ T_{FH} subsets. Representative plots (left) and pooled data (right) (n = 22). Error bars represent means ± SEM. Paired t test and Wilcoxon matched-pairs signed-rank test were applied to the BCL6 and CD45RO graphs, respectively. (**C**) Histograms of the distribution of BCL6 and CD45RO among ICOS$^-$PD-1$^-$ T_{FH} cells (orange) and ICOS$^+$PD-1$^+$ T_{FH} cells (blue). (**D**) Visualization of the PCA from the fluorescence values of each flow cytometry marker from one tonsil. Cell subsets in the PCA are colored as indicated. (**E**) Percentage of variance of the data explained by the first five principal components (left) and heatmap of the correlation values for each of the markers explained by PC1 (right).

ICOS$^+$PD-1$^+$ T_{FR} cells are located specifically within the GC

To consolidate our previous findings, confocal images were acquired from human tonsils. As expected, PD-1 was highly expressed in the GC (Fig. 4A). In line with the hypothesis that PD-1 expression is restricted to the most mature T_{FR} cells, we found few PD-1$^+$ cells among the FOXP3$^+$ T_{FR} cells, but those PD-1$^+$ T_{FR} cells also expressed ICOS and were located within the GC (Fig. 4, B and C, and fig. S5). Conversely, FOXP3$^+$ cells found outside the GC, namely, in the follicle, were either ICOS$^+$ or did not express either ICOS or PD-1 (Fig. 4, B and C, and fig. S5). These findings align with our earlier observations using flow cytometry indicating that ICOS$^+$PD-1$^+$ T_{FR} cells are a minor population, which likely represent the most mature subset, and are therefore primarily located within the GC (Fig. 4D). Whereas a substantial proportion of FOXP3$^+$ cells in the GC are ICOS$^-$PD-1$^-$, the ICOS$^+$PD-1$^+$ subset is enriched in the GC, supporting the notion that their maturation is associated with this specific location.

The tonsil CD4$^+$CD25$^+$CXCR5^{int}ICOS^{int} population contains a high frequency of FOXP3$^+$ cells, representing an innovative approach to isolating T_{FR} cells from human lymphoid tissue

Whereas human circulating T_{FR} cells can be readily isolated based on the expression of CXCR5 and CD25 (*27*), the isolation of T_{FR} cells from human lymphoid tissue has been challenging and an obstacle in studying their suppressive function. No unique extracellular markers are known to define lymphoid tissue T_{FR} cells unequivocally allowing the isolation of a pure T_{FR} cell population (containing a high frequency of FOXP3$^+$ cells). Our data on the expression of ICOS and PD-1 described above prompted us to explore alternative strategies to isolate T_{FR} cells from human tissue.

The most common way to isolate human T_{FR} cells from lymphoid tissue relies on the selection of CD4$^+$CD25$^+$CXCR5^{hi}ICOS^{hi} cells. Nevertheless, human tonsils contain a very low percentage of CD25$^+$ cells among the CD4$^+$CXCR5^{hi}ICOS^{hi} cells (Fig. 5A) and, within those, only ~20% of the cells are positive for FOXP3 (Fig. 5B), leading to very few "true" T_{FR} cells (i.e., FOXP3$^+$ cells) isolated using this gating strategy. In addition, this strategy does not exclude the CD25$^+$FOXP3$^-$ IL-10 TF cells, which also have suppressive function, and are numerically similar to the T_{FR} cells in this population (*11*, *18*). Furthermore, despite the abundance of ICOS, most T_{FR} cells do not express high levels of CXCR5; instead, they express intermediate levels (fig. S7). Consequently, although selecting CXCR5^{hi} cells allows capturing the most mature T_{FR} cells (albeit among many "contaminant" Foxp3$^-$ cells), this strategy would not yield a representative proportion of the global T_{FR} cell population. Alternatively, based on our previous observations, CD4$^+$CXCR5^{int}ICOS^{int} cells contain a considerably higher percentage of CD25$^+$ cells (Fig. 5A), which, in turn, is reflected in a markedly higher proportion of selected FOXP3$^+$ cells (Fig. 5B). Thus, we propose to select CD4$^+$CD25$^+$

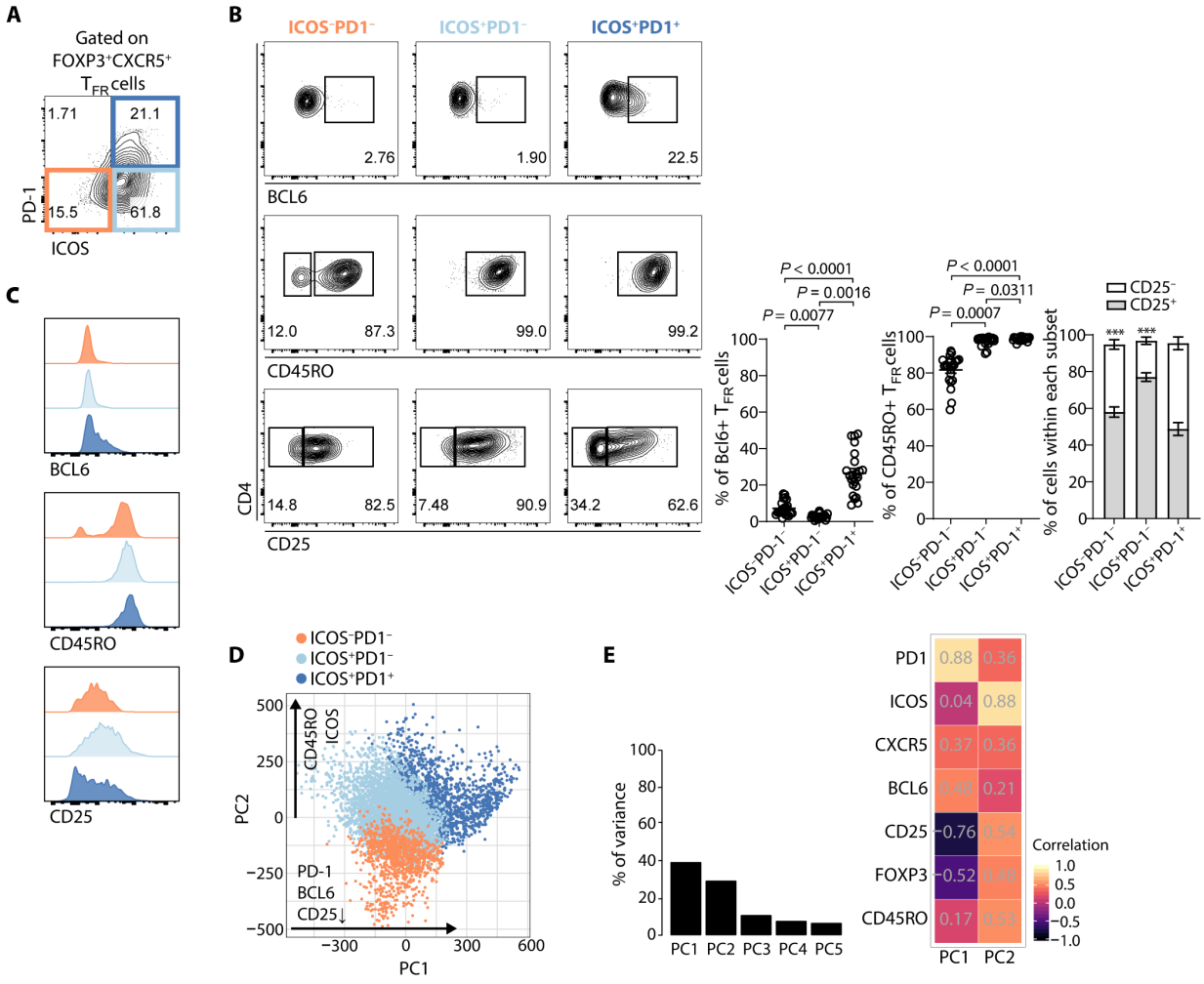

Fig. 3. The ICOS$^+$PD-1$^-$ population represents T_{FR} cells in an intermediate maturation stage. (**A**) Representative contour plot showing the identification of ICOS$^-$PD-1$^-$ (orange), ICOS$^+$PD-1$^-$ (light blue), and ICOS$^+$PD-1$^+$ (blue) subsets of tonsil CD4$^+$FOXP3$^+$CXCR5$^+$ T_{FR} cells by flow cytometry. (**B**) Frequency of cells expressing BCL6, CD45RO, and CD25 within the ICOS$^-$PD-1$^-$, ICOS$^+$PD-1$^-$, and ICOS$^+$PD-1$^+$ T_{FR} subsets. Representative plots (left) and pooled data (right) are shown (n = 22). Error bars represent means ± SEM. Friedman test with Dunn's multiple comparisons test was applied to the BCL6 and CD45RO graphs. For CD25 analysis, ***P < 0.001 using two-way ANOVA with Bonferroni's multiple comparison test. (**C**) Histograms of BCL6, CD45RO, and CD25 distribution among ICOS$^-$PD-1$^-$ T_{FR} cells (orange), ICOS$^+$PD-1$^-$ T_{FR} cells (light blue), and ICOS$^+$PD-1$^+$ T_{FH} cells (blue). (**D**) Visualization of the PCA from fluorescence values of each flow cytometry marker. The position of the T_{FR} cells from the three subsets within the PCA is indicated by color. (**E**) Percentage of variance of the data explained by the first five principal components (left) and heatmap of the correlation values for each marker explained by PC1 and PC2 (right).

CXCR5^{int}ICOS^{int} cells to isolate from human lymphoid tissue a population with a greater purity of T_{FR} cells (assessed by the frequency of the FOXP3-expressing cells in the sorted population) and a better yield of T_{FR} cells (Fig. 5B).

The proposed strategy offers a significant improvement in isolating T_{FR} cells with intermediate levels of CXCR5 expression. This approach may result in the exclusion of cells with higher CXCR5 expression, which also exhibit elevated levels of ICOS, PD-1, and BCL6. This excluded subset represents a minor yet critical population, encompassing the most mature CD25$^-$ T_{FR} cells. The generally used gating strategy, by selecting CD4$^+$CD25$^+$CXCR5^{hi}ICOS^{hi} cells, contains a substantial proportion of the recently described IL-10–producing T follicular (IL-10 TF) cells (*11*, *18*). Although IL-10 TF cells lack FOXP3 expression, they differ from prototypic T_{FH} cells by expressing CD25 (Fig. 5C). However, IL-10 TF cells closely resemble FOXP3$^+$CXCR5^{hi} T_{FR} cells in terms of the presence of ICOS and PD-1 (Fig. 5D), as well as their regulatory function of suppressing T cell proliferation mediated by IL-10 (*18*). Therefore, given the increased frequency of FOXP3$^-$ cells (Fig. 5B), targeting the CD4$^+$CD25$^+$CXCR5^{hi}ICOS^{hi} cell population appears to be a promising strategy for isolating IL-10 TF cells.

The most mature FOXP3$^+$CXCR5^{hi} T_{FR} cells show higher expression of BCL6 and less expression of CD25 compared to FOXP3$^+$CXCR5^{int} T_{FR} cells (Fig. 5D). These observations are consistent with previous studies suggesting that lymphoid tissue T_{FR} cells downregulate CD25 and increase CXCR5 expression as they mature, both in mice and humans (*23*, *24*). However, CD25 needs to be used in a T_{FR} cell isolation strategy based on CXCR5 and ICOS markers to exclude the T_{FH} cells (CD25$^-$) that are present in vast excess within the CXCR5^{hi}ICOS^{hi} gate. Consequently, the most mature CD25$^-$ T_{FR} cells are also absent from a sorting strategy based on CXCR5^{hi}ICOS^{hi} cells. In conclusion, although an ideal approach for isolating mature

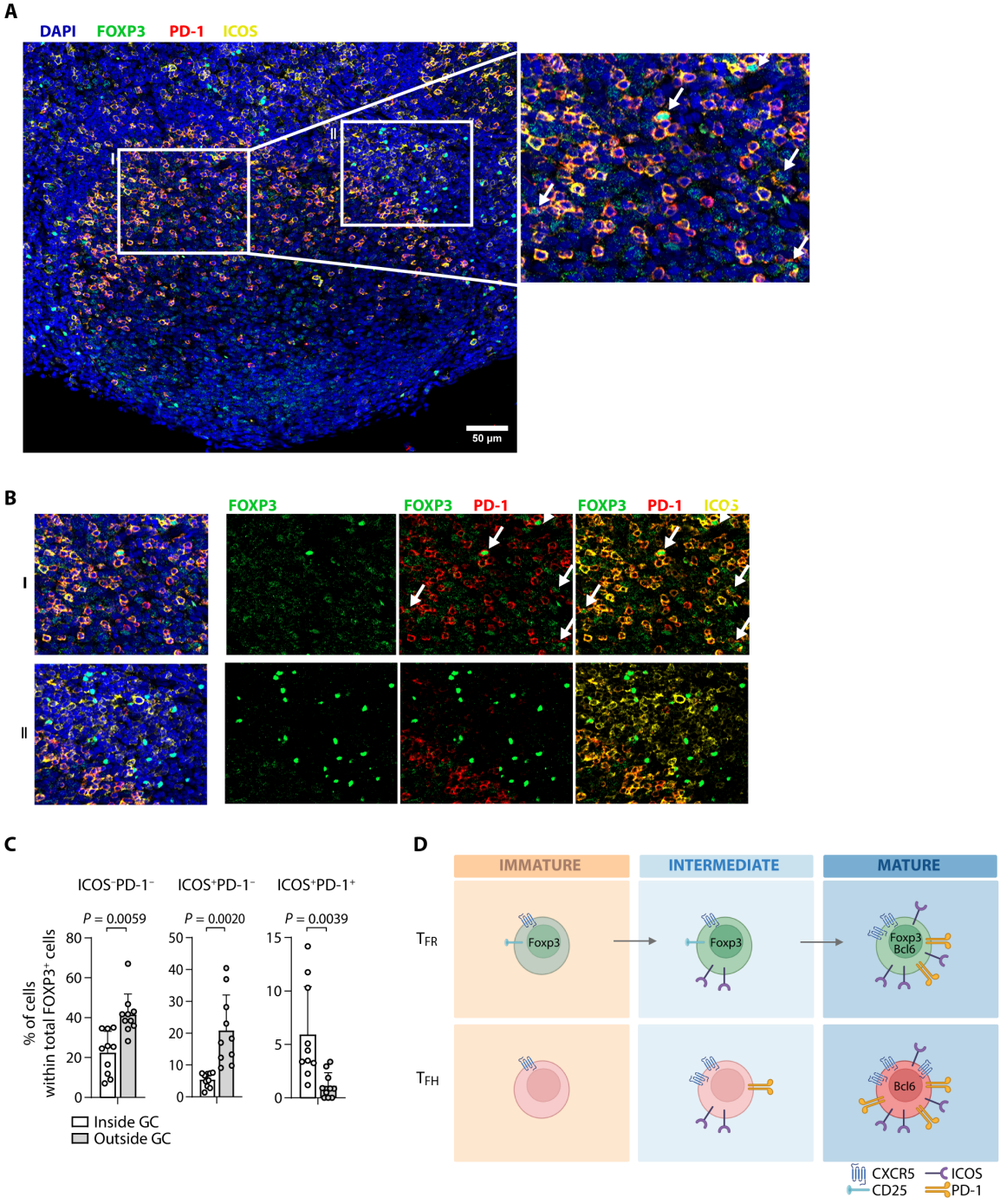

Fig. 4. ICOS$^+$PD-1$^+$ T_{FR} cells localize specifically within the GC. (**A**) Representative image of the immunofluorescence microscopy of human tonsils stained for DAPI (blue), FOXP3 (green), ICOS (yellow), and PD-1 (red). Individual image panels were stitched together to reconstruct the full sample area using tile imaging and *z*-stack acquisition. Outlined area I is represented as an enlarged image on the right, in which ICOS$^+$PD-1$^+$FOXP3$^+$ cells are identified (white arrows). (**B**) Outlined areas I and II indicated in (A). Data are representative of tonsil sections from four healthy children (see fig. S6 for another example). (**C**) Quantification of ICOS$^-$PD-1$^-$, ICOS$^+$PD-1$^-$, and ICOS$^+$PD-1$^+$ T_{FR} cells within (white bars) and outside (gray bars) the GC. Data are pooled from two to three images per tonsil of four healthy children (n = 10). Error bars represent means ± SEM. Wilcoxon matched-pairs signed-rank test was applied. (**D**) Model of T_{FH} and T_{FR} cell maturation in human tissue, given by the expression of ICOS, PD-1, CXCR5, BCL6, and CD25. Created in BioRender. I. Biorender (2025), https://BioRender.com/1cjps16.

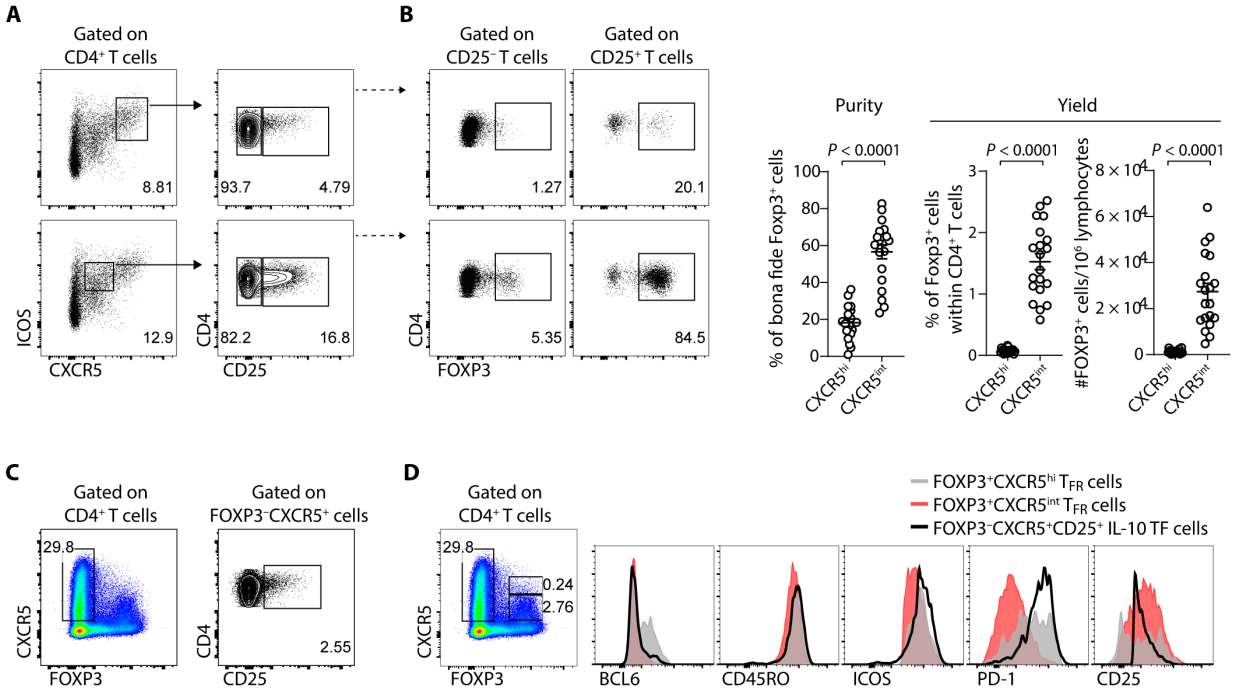

Fig. 5. The CD4$^+$CD25$^+$CXCR5^{int}ICOS^{int} cell population from human tonsils contains a high frequency of FOXP3$^+$ cells. (**A**) Comparison of two alternative gating strategies used for sorting T_{FR} cells from lymphoid tissue, selecting either CXCR5^{hi}ICOS^{hi} cells (top; conventional strategy) or CXCR5^{int}ICOS^{int} cells (bottom; proposed strategy). (**B**) Analysis of the frequency of FOXP3$^+$ T_{FR} cells within the hypothetical isolated population using the strategies described in (A): CXCR5^{hi}ICOS^{hi}CD25$^-$ (top left), CXCR5^{hi}ICOS^{hi}CD25$^+$ (top right), CXCR5^{int}ICOS^{int}CD25$^-$ (bottom left), and CXCR5^{int}ICOS^{int}CD25$^+$ (bottom right). Representative plots (left) and pooled data (right) ($n = 20$). Error bars represent means ± SEM. Paired *t* test was applied. (**C**) Representative plots showing CD4$^+$FOXP3$^-$CXCR5$^+$CD25$^+$ IL-10 TF cells. (**D**) Expression of BCL6, CD45RO, ICOS, PD-1, and CD25 by CXCR5^{hi} T_{FR} cells (gray), CXCR5^{int} T_{FR} cells (red), and IL-10 TF cells from human tonsils (black line).

CD25$^-$ T_{FR} cells remains to be defined, the proposed strategy based on CD4$^+$CD25$^+$CXCR5^{int}ICOS^{int} greatly increases the purity and number of T_{FR} cells isolated from human lymphoid tissue, although with a bias toward capturing the intermediate maturation stages.

Lymphoid tissue T_{FR} cells have greater suppressive function than circulating T_{FR} cells

To address the suppressive function of lymphoid tissue T_{FR} cells, we performed in vitro cocultures to measure their ability to suppress B cell activation and T_{FH} cell proliferation. We performed the same assays with circulating T_{FR} cells. We found that, in line with what was previously reported both in mice and humans (*27*, *28*), circulating T_{FR} cells (isolated as CD4$^+$CD25$^+$CXCR5$^+$) can suppress B cell activation, as measured by CD38 up-regulation, and T_{FH} cell proliferation (Fig. 6A). Tonsil T_{FR} cells were sorted from the tissue using the strategy described above, as CD4$^+$CD25$^+$CXCR5^{int} ICOS^{int}. Therefore, we anticipate a bias toward an intermediate maturation stage (and not including the most mature CD25$^-$ T_{FR} cells), but in the absence of the putative contaminating CD25$^+$ IL-10 TF cells. We found that the lymphoid tissue T_{FR} cells can suppress the activation of B cells and proliferation of T_{FH} cells (Fig. 6B). Furthermore, the tonsil T_{FR} cells, even devoid of the most mature population, could suppress the proliferation of T_{FH} cells more efficiently than circulating T_{FR} cells (Fig. 6C).

DISCUSSION

There is limited knowledge regarding the differentiation and function of human T_{FR} cells within lymphoid tissue. Our results show that ICOS and PD-1 are useful surface markers to distinguish different developmental states of T_{FR} cells. These regulatory cells up-regulate ICOS and PD-1 in a sequential way as they mature: In an intermediate maturation stage, T_{FR} cells display ICOS in the absence of PD-1, whereas only the most mature T_{FR} cells coexpress both ICOS and PD-1.

We examined a panel of 50 human tonsils with a comprehensive flow cytometry approach to characterize the expression of ICOS and PD-1 on the maturation of T_{FH} and T_{FR} cells. We identified three main subsets of T_{FR} cells—PD-1$^-$ICOS$^-$, PD-1$^-$ICOS$^+$, and PD-1$^+$ICOS$^+$—with different characteristics regarding the expression of canonical follicular and GC markers. This observation is markedly distinct from what is observed in T_{FH} cells, where we found a strong linear correlation between cells expressing PD-1 and those expressing ICOS. The correlation is so precise that the two molecules can be used interchangeably to define the maturation trajectory of T_{FH} cells. The PCA further supports a linear maturation of T_{FH} cells: At their most immature stage, T_{FH} cells are PD-1$^-$ICOS$^-$, and they acquire PD-1, ICOS, and BCL6 in a coordinated throughout the maturation process. Our previous work using a pseudo-time algorithm to infer the developmental trajectory of human T_{FH} cells based on single-cell transcriptomics datasets showed that the increase in gene expression of ICOS and PDCD1 (PD-1) occurs almost simultaneously (*19*).

The maturation of human T_{FR} cells seems to have another layer of complexity. The distribution of the analyzed proteins along the T_{FR} maturation trajectory is not linear, as suggested by our PCA. The lack of expression of the GC marker BCL6 suggests that PD-1$^-$ICOS$^-$ T_{FR} cells have an immature phenotype similar to that described for their counterparts in blood (*27*). Conversely, the PD-1$^+$ICOS$^+$ subset of T_{FR}

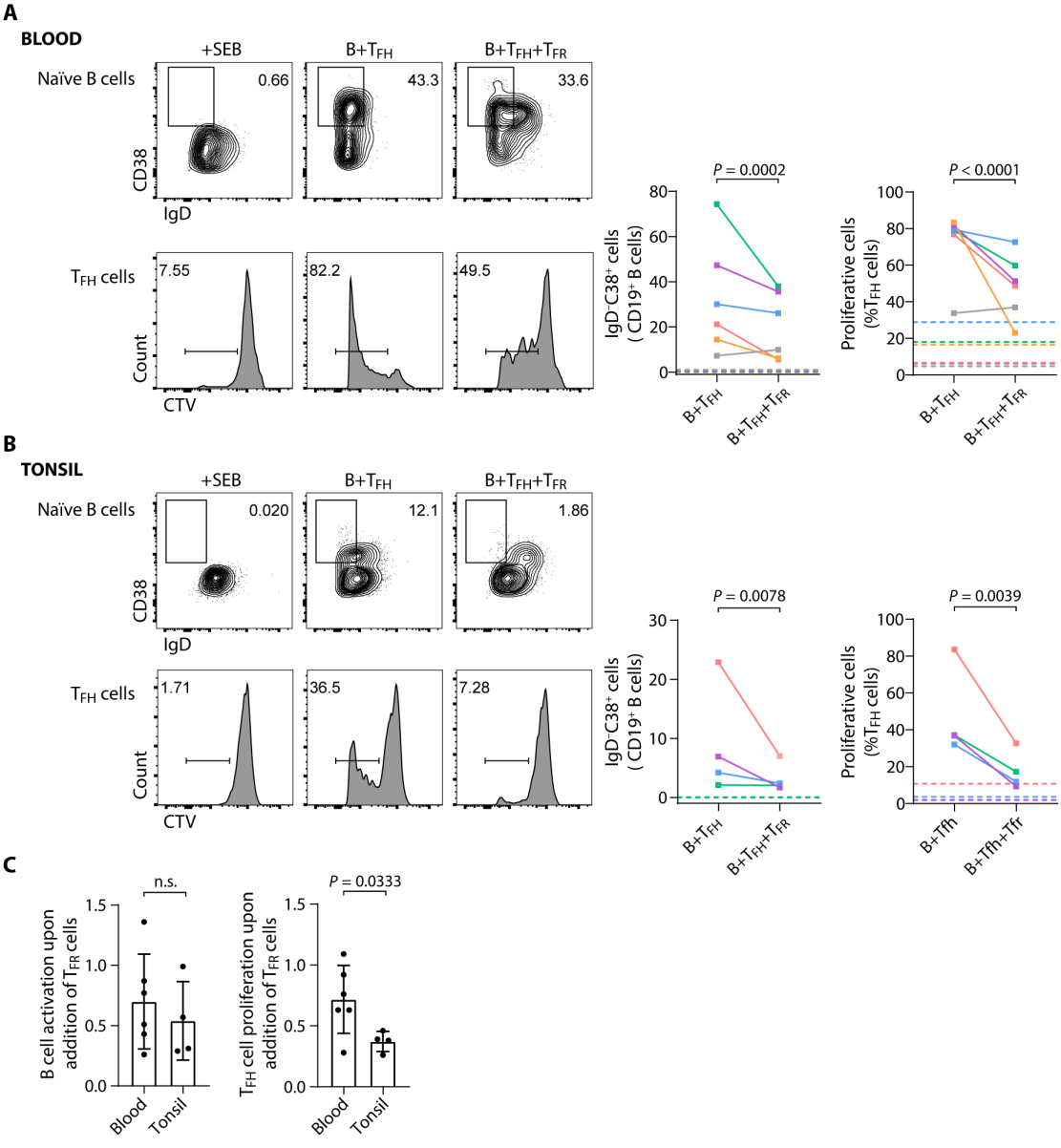

Fig. 6. Suppressive function of circulating and tonsil T_{FR} cells. To assess the suppressive capacity of T_{FR} populations, cocultures of T_{FR} cells (from peripheral blood or human tonsils) with naïve B cells and T_{FH} cells from the same donor were assessed after 5 days of stimulation with SEB. (**A**) In cultures with T_{FR} cells isolated from the peripheral blood (sorted as $CD4^+CD25^+CXCR5^+$), up-regulation of CD38 and down-regulation of IgD by naïve B cells (top) and proliferation of T_{FH} cells measured by CTV dilution (bottom) were analyzed. Representative plots (left) and pooled data (right) are shown ($n = 6$). (**B**) In cocultures of tonsil T_{FR} cells (sorted as $CD4^+CD25^+ICOS^{int}CXCR5^{int}$), up-regulation of CD38 and down-regulation of IgD by naïve B cells (top) and proliferation of T_{FH} cells measured by CTV dilution (bottom) were analyzed. Representative plots (left) and pooled data (right) are shown ($n = 4$). In (A) and (B), each donor is represented by a unique color and each dot represents the mean of technical replicates within the same donor. Horizontal dashed lines represent controls (B cells + SEB; or T_{FH} + SEB). Statistical significance was assessed using the Wilcoxon matched-pairs signed-rank test. (**C**) Comparison of the ability of T_{FR} cells isolated from the peripheral blood and human tonsil to suppress B cell activation and T_{FH} cell proliferation, applying the ratio between cocultures with and without T_{FR} cells described above [$(B+T_{FH}+T_{FR}):(B+T_{FH})$] ($n = 6$ for blood and $n = 4$ for tonsil; unpaired Mann-Whitney *U* test); n.s., not significant.

cells can be considered as the most mature, given the abundance of BCL6 and CD45RO, but not CD25. CD25 is lost in the most mature GC T_{FR} cells (*19*, *23*, *24*). Nevertheless, numerically, very few cells correspond to the most mature $CD25^-$ T_{FR} population displaying high levels of both ICOS and PD-1. This finding aligns with the research conducted by Sayin and colleagues, who demonstrated that, in contrast to T_{FH} cells, most T_{FR} cells in human mesenteric lymph nodes do not express PD-1 (*13*). Furthermore, they observed that PD-1^+ T_{FR} cells exhibited higher levels of ICOS (*13*). Our previous observations in tonsil, using single-cell RNA sequencing, also support this pattern as the small proportion of T_{FR} cells found to express PDCD1 (PD-1) likely represented the most mature T_{FR} cells (*19*).

T_{FR} cells in an intermediate maturation stage express ICOS but little PD-1. A recent study in mice has demonstrated that ICOS is

required for generation of T_{FR} cells by indirectly promoting the expression of BCL6 and CXCR5, proving to be essential in the early stages of T_{FR} cell development (*29*). In addition, ICOS may also be important in the later stages of T_{FR} cell function, as supported by research demonstrating that blocking its signaling results in the expansion of autoreactive B cells and increased autoantibody titers (*29*). Conversely, PD-1 inhibits the activation and proliferation of T_{FR} cells in mouse lymph nodes and blood, thereby suppressing the immune response (*30*). In addition, PD-1 expression in the GC seems of utmost importance because it regulates selection and survival, affecting the quantity and quality of long-lived plasma cells (*31*). Although these studies were conducted in mice, they suggest that T_{FR} cells can regulate the immune response by limiting excessive B cell responses and preventing autoimmunity through PD-1. These observations highlight the potential functional significance of the acquisition of PD-1 by fully mature T_{FR} cells.

The distinct location of T_{FR} cells at different maturation stages within the follicle holds key importance. A previous study revealed that PD-1^+ T_{FH} cells were particularly enriched in GCs, but the relationship between PD-1 surface expression and T_{FR} cell location was less evident (*13*). In addition, it was reported that PD-1^+ T_{FR} cells display superior IL-10 production compared to PD-1^- T_{FR} cells and T_{reg} cells (*13*). Here, we show that $ICOS^+$PD-1^+ T_{FR} cells, as the most mature population, preferentially locate within the GC whereas T_{FR} cells lacking PD-1 expression are mostly found outside the GC.

Part of the limited understanding of T_{FR} cell function in humans can be attributed to the challenge of isolating these cells for in vitro functional studies as there are no known surface proteins allowing their precise sorting. Our findings on PD-1 and ICOS expression led us to explore an alternative strategy for flow cytometry isolation of T_{FR} cells. By selecting $CD4^+CD25^+CXCR5^{int}ICOS^{int}$ T_{FR} cells, we were able to obtain a significantly enriched population in $FOXP3^+$ T_{FR} cells and devoid of $CD25^+$ IL-10 TF cells to assess the suppressive function of tissue T_{FR} cells in vitro. We found that tonsil T_{FR} cells have greater suppressive function than circulating T_{FR} cells. These observations are consistent with a previous study showing that circulating T_{FR} cells, being immature, are not yet fully competent in their suppressive ability (*27*). Recently, CD38 was shown to discriminate T_{FH}-derived T_{FR} cells from T_{reg}-derived T_{FR} cells (*10*). Although the $CD38^+$ T_{FH}-derived T_{FR} cells represent only about 30% of the overall T_{FR} population, they comprise about 70% of the T_{FR} cells in the GC and only 7% of the T_{FR} cells in the B cell follicle (*10*) while maintaining CD25 expression. Thus, it is possible to use CD38 to further improve the identification strategy of GC T_{FR} cells reported in this study as the vast majority of the T_{FR} cells that our method targets do not contain GC-resident cells. Nevertheless, a strategy for specifically capturing the most mature GC–resident $CD25^-$ T_{FR} cells has yet to be established.

Overall, our results show that the close resemblance in surface receptors between T_{FH} and T_{FR} cells does not necessarily imply a parallel pattern of maturation for both cell types. Notably, the acquisition of CXCR5, ICOS, and PD-1 exhibits divergent trends along their maturation processes. The distinct usage of ICOS and PD-1 may provide an opportunity for selectively targeting T_{FR} cells at different stages of maturation.

MATERIALS AND METHODS

Experimental design

We hypothesized that the maturation of T_{FH} and T_{FR} cells follow distinct pathways. To investigate this, we studied these cell populations in human tonsils with the aim of elucidating their maturation processes through proteins previously known to be expressed by T_{FH} and T_{FR} cells. We used flow cytometry combined with a bioinformatics approach, specifically PCA, to analyze the dynamics of the proteins included in our staining panel simultaneously. Our initial observations indicated that the maturation of T_{FH} and T_{FR} cells, as assessed by the expression of PD-1 and ICOS, occurs in different patterns. To further validate these findings, we performed confocal imaging to confirm the spatial localization of distinct T_{FR} cell subsets: $ICOS^-$PD-1^-, $ICOS^+$PD-1^-, and $ICOS^+$PD-1^+. Because of the challenge of isolating T_{FR} cells from human tissues—largely owing to the lack of specific extracellular markers—and in light of our findings on the distinct maturation trajectories of T_{FH} and T_{FR} cells (based on PD-1 and ICOS expression), we developed an alternative sorting strategy. This method enables the isolation of a purer and more abundant population of T_{FR} cells from human lymphoid tissues.

Human samples

Tonsils were collected from children submitted to tonsillectomy due to tonsil hypertrophy ($n = 50$, 3.8 ± 1.9 years old, 24 females and 26 males). Children with additional clinical conditions, or under any drug treatment, were excluded. The studies were approved by the Lisbon Academic Medical Center Ethics Committee (reference no. 548/14). Informed consent was obtained from all adult volunteers, parents, or legal guardians.

Cell isolation

Lymphocytes from tonsils were isolated using Ficoll gradient medium (Histopaque-1077; Sigma-Aldrich) after mechanical disruption. Peripheral blood mononuclear cells (PBMCs) were isolated from buffy coats by Ficoll gradient medium using SepMate tubes (StemCell Technologies). Samples for cell sorting were previously treated with the MojoSort Human CD4 T Cell Isolation Kit (BioLegend) to separate CD4 T cell fractions: The CD4+ fraction was used to isolate CD4+ T cell subsets, whereas the $CD4^-$ fraction was used to isolate naïve B cells (see fig. S8 for sorting strategy).

Cell sorting and flow cytometry analysis

PBMCs and lymphocytes from tonsils were stained with the following antibodies for cell sorting and/or flow cytometry analysis: anti-CD4 (OKT4, BioLegend), anti-CD45RO (UCHL1, BioLegend), anti-CD185/CXCR5 (J252D4, BioLegend), anti-CD279/PD-1 (EH12.2H7, BioLegend), anti-CD278/ICOS (C398.4A, BioLegend), anti-CD27 (M-T271, BioLegend), anti-IgD (IA6-2, BioLegend), anti-CD38 (HB-7, BioLegend), anti-CD25 (BC96, Thermo Fisher Scientific), anti-CD127 (eBioRDR5, eBioscience), anti-CD19 (HIB19, eBioscience), anti-FOXP3 (PCH101, Thermo Fisher Scientific), and anti-BCL6 (K112-91, BD Biosciences). The Live/Dead Fixable Aqua Dead Stain Kit (Life Technologies) was used for exclusion of dead cells. Intracellular FOXP3 and BCL6 staining was performed using the FOXP3 Fix/Perm Kit (Thermo Fisher Scientific) according to the manufacturer's instructions. Samples were acquired on a BD LSRFortessa cytometer (BD Biosciences) and further analyzed on the FlowJo software v.10.5.3 (TreeStar). Cell sorting was performed in a BD FACSAria Fusion instrument (BD Biosciences).

Functional assays

For the in vitro functional assays, 30×10^3 naïve B cells ($CD19^+IgD^+CD27^-$) were cultured with 25×10^3 T_{FH} cells (sorted

as $CD4^+CD127^+CD25^-CXCR5^+$ in the blood and $CD4^+CD25^-CXCR5^+ICOS^+$ in the tonsil) and 25×10^3 T_{FR} cells (sorted as $CD4^+CD127^-CD25^+CXCR5^+$ in blood and $CD4^+CD25^+CXCR5^{int}ICOS^{int}$ in tonsil). Cells were cultured with SEB (1 μg/ml) (Sigma-Aldrich). Cells were plated in U-bottom 96-well plates in RPMI 1640 (Life Technologies) supplemented with 10% heat-inactivated fetal bovine serum (Life Technologies), 1% Hepes (Sigma-Aldrich), 1% sodium pyruvate (Life Technologies), 1% penicillin-streptomycin (Life Technologies), and 0.05% gentamicin (Life Technologies) under 37°C and 5% CO_2 incubator conditions. After 5 days, proliferation of T_{FH} cells was analyzed by using the CellTrace Violet (CTV) Proliferation Kit (Invitrogen) and differentiation of B cells was assessed through the up-regulation of CD38 by flow cytometry. For these functional assays, six biological replicates were used for the buffy coat experiments and four biological replicates for the tonsil experiments. Triplicates were performed for each biological replicate whenever cell numbers allowed. When cell numbers were limited, fewer technical replicates were conducted.

Bioinformatics analysis

Fluorescence values were extracted for each marker (ICOS, PD-1, CD25, CXCR5, CD45RO, BCL6, and FOXP3) from flow cytometry data from tonsils by using the FlowJo software v.10.5.3 (TreeStar). For each tonsil, these values were extracted separately from different populations of T_{FH} and T_{FR} cells, as follows: $PD\text{-}1^-ICOS^-$, $PD\text{-}1^-ICOS^+$, $PD\text{-}1^+ICOS^-$, and $PD\text{-}1^+ICOS^+$ subsets. Further analysis was performed individually for each tonsil using the software RStudio (see fig. S9 for PCA in different tonsils). Principal components were calculated using the prcomp() function. Correlation matrices were calculated using the cor() function. Visualization of PCA and correlations was done by using the ggplot2 package. The analysis of T_{FH} cells combined $PD\text{-}1^-ICOS^-$ and $PD\text{-}1^+ICOS^+$ subsets, whereas for T_{FR} cells, the analysis included $PD\text{-}1^-ICOS^-$, $PD\text{-}1^-ICOS^+$, and $PD\text{-}1^+ICOS^+$ subsets (refer to fig. S10 for the combined analysis of T_{FH} and T_{FR} cells, irrespective of PD-1/ICOS subsets). This analysis was performed using R v.4.1.1.

Immunofluorescence

Three-micrometer sections of formalin-fixed paraffin-embedded human tonsil were deparaffinized and submitted to antigen retrieval by heat (PT link pretreatment module for tissue specimens, Thermo Fisher Scientific at pH 9, Leica Biosystems). Background reduction was applied by incubation with 3% H_2O_2 (Sigma-Aldrich) in methanol. Total protein block was also applied (Dako). Then, sections were stained with anti-human FOXP3 (PCH101, Thermo Fisher Scientific), anti-human ICOS (D1K2T, Cell Signaling), and anti-human PD-1 (NAT105, BioLegend) primary antibodies. Anti-rat AF488 (Thermo Fisher Scientific), anti-rabbit AF546 (Thermo Fisher Scientific), and anti-mouse AF647 (Thermo Fisher Scientific) were used as secondary antibodies, respectively. Cell nuclei were visualized with 4′,6-diamidino-2-phenylindole (DAPI). Images were acquired on a Zeiss LSM 980 point-scanning confocal microscope with Airyscan 2, using a Plan-Apochromat 20x/0.8 objective (pixel size: 124 nm). Tile imaging and *z*-stack acquisition were used to cover the entire volume of interest. The tiled images were stitched together to reconstruct the full sample area, and subsequently, a maximum intensity projection was applied to generate a two-dimensional representation of the three-dimensional data. Cell counting was performed using software developed in-house, written in MATLAB (MathWorks, Natick, MA). Briefly, single cells were segmented and labeled with a pretrained Cellpose deep learning model (*32*) using the DAPI channel, and subsequent combinatorial filters for cell counting were defined on the basis of staining (e.g., positive staining in FOXP3 and ICOS channels but not in the PD-1 channel or positive staining in FOXP3, ICOS, and PD-1 channels), where a staining was considered positive if a minimum number of pixels were above a given threshold. Individual report images with segmentation and filtering results were also generated by the software for cell counting verification. GC boundaries were defined based on cell density as visualized by DAPI nuclear staining (fig. S11).

Statistical analysis

The Shapiro-Wilk normality test was applied to assess the normality of the data distribution. For comparisons between two groups, the paired *t* test was used if data passed the normality test. If the data did not meet the normality assumption, the Wilcoxon matched-pairs signed-rank test was applied. For pairwise multiple comparisons, either the Friedman test with Dunn's multiple comparisons test or the two-way analysis of variance (ANOVA) with Bonferroni's multiple comparison test were applied. For the functional assays, the Wilcoxon matched-pairs signed-rank test was used to assess statistical significance within the blood and tonsil, whereas the unpaired Mann-Whitney *U* test was applied to assess differences between compartments. *P* values less than 0.05 were considered significant. Graphs were prepared using GraphPad Prism v.8.4.3 software, and statistical analysis was performed using GraphPad Prism v.8.4.3 and R studio v.4.3.0.

Supplementary Materials

The PDF file includes:

Figs. S1 to S11
Table S1
Legend for table S2

Other Supplementary Material for this manuscript includes the following:

Table S2

REFERENCES AND NOTES

1. S. Crotty, A brief history of T cell help to B cells. *Nat. Rev. Immunol.* **15**, 185–189 (2015).
2. Y. Chung, S. Tanaka, F. Chu, R. I. Nurieva, G. J. Martinez, S. Rawal, Y. H. Wang, H. Lim, J. M. Reynolds, X. H. Zhou, H. M. Fan, Z. M. Liu, S. S. Neelapu, C. Dong, Follicular regulatory T cells expressing Foxp3 and Bcl-6 suppress germinal center reactions. *Nat. Med.* **17**, 983–988 (2011).
3. M. A. Linterman, W. Pierson, S. K. Lee, A. Kallies, S. Kawamoto, T. F. Rayner, M. Srivastava, D. P. Divekar, L. Beaton, J. J. Hogan, S. Fagarasan, A. Liston, K. G. C. Smith, C. G. Vinuesa, $Foxp3^+$ follicular regulatory T cells control the germinal center response. *Nat. Med.* **17**, 975–982 (2011).
4. I. Wollenberg, A. Agua-Doce, A. Hernandez, C. Almeida, V. G. Oliveira, J. Faro, L. Graca, Regulation of the germinal center reaction by $Foxp3^+$ follicular regulatory T cells. *J. Immunol.* **187**, 4553–4560 (2011).
5. W. Fu, X. Liu, X. Lin, H. Feng, L. Sun, S. Li, H. Chen, H. Tang, L. Lu, W. Jin, C. Dong, Deficiency in T follicular regulatory cells promotes autoimmunity. *J. Exp. Med.* **215**, 815–825 (2018).
6. P. T. Sage, A. H. Sharpe, T follicular regulatory cells in the regulation of B cell responses. *Trends Immunol.* **36**, 410–418 (2015).
7. M. Aloulou, E. J. Carr, M. Gador, A. Bignon, R. S. Liblau, N. Fazilleau, M. A. Linterman, Follicular regulatory T cells can be specific for the immunizing antigen and derive from naive T cells. *Nat. Commun.* **7**, 10579 (2016).
8. A. R. Maceiras, S. C. P. Almeida, E. Mariotti-Ferrandiz, W. Chaara, F. Jebbawi, A. Six, S. Hori, D. Klatzmann, J. Faro, L. Graca, T follicular helper and T follicular regulatory cells have different TCR specificity. *Nat. Commun.* **8**, 15067 (2017).
9. J. T. Jacobsen, W. Hu, T. B. R. Castro, S. Solem, A. Galante, Z. Lin, S. J. Allon, L. Mesin, A. M. Bilate, A. Schiepers, A. K. Shalek, A. Y. Rudensky, G. D. Victora, Expression of Foxp3 by T follicular helper cells in end-stage germinal centers. *Science* **373**, eabe5146 (2021).
10. C. Le Coz, D. A. Oldridge, R. S. Herati, N. De Luna, J. Garifallou, E. Cruz Cabrera, J. P. Belman, D. Pueschl, L. V. Silva, A. V. C. Knox, W. Reid, S. Yoon, K. B. Zur, S. D. Handler, H. Hakonarson,

E. J. Wherry, M. Gonzalez, N. Romberg, Human T follicular helper clones seed the germinal center–resident regulatory pool. *Sci. Immunol.* **8**, eade8162 (2023).
11. L. Graca, J. Jacobsen, S. Kumar, The expanding family of T follicular regulatory cells. *Sci. Immunol.* **8**, eadg7526 (2023).
12. N. M. Haynes, C. D. C. Allen, R. Lesley, K. M. Ansel, N. Killeen, J. G. Cyster, Role of CXCR5 and CCR7 in follicular Th cell positioning and appearance of a programmed cell death gene-1 high germinal center-associated subpopulation. *J. Immunol.* **179**, 5099–5108 (2007).
13. I. Sayin, A. J. Radtke, L. A. Vella, W. Jin, E. J. Wherry, M. Buggert, M. R. Betts, R. S. Herati, R. N. Germain, D. H. Canaday, Spatial distribution and function of T follicular regulatory cells in human lymph nodes. *J. Exp. Med.* **215**, 1531–1542 (2018).
14. Y. S. Choi, R. Kageyama, D. Eto, T. C. Escobar, R. J. Johnston, L. Monticelli, C. Lao, S. Crotty, ICOS receptor instructs T follicular helper cell versus effector cell differentiation via induction of the transcriptional repressor Bcl6. *Immunity* **34**, 932–946 (2011).
15. H. Xu, X. Li, D. Liu, J. Li, X. Zhang, X. Chen, S. Hou, L. Peng, C. Xu, W. Liu, L. Zhang, H. Qi, Follicular T-helper cell recruitment governed by bystander B cells and ICOS-driven motility. *Nature* **496**, 523–527 (2013).
16. J. Shi, S. Hou, Q. Fang, X. X. Liu, X. X. Liu, H. Qi, PD-1 controls follicular T helper cell positioning and function. *Immunity* **49**, 264–274.e4 (2018).
17. V. R. Fonseca, F. Ribeiro, L. Graca, T follicular regulatory (Tfr) cells: Dissecting the complexity of cell compartments. *Immunol. Rev.* **288**, 112–127 (2019).
18. P. F. Cañete, R. A. Sweet, P. Gonzalez-Figueroa, I. Papa, N. Ohkura, H. Bolton, J. A. Roco, M. Cuenca, K. J. Bassett, I. Sayin, E. Barry, A. Lopez, D. H. Canaday, M. Meyer-Hermann, C. Doglioni, B. Fazekas de St Groth, S. Sakaguchi, M. C. Cook, C. G. Vinuesa, Regulatory roles of IL-10–producing human follicular T cells. *J. Exp. Med.* **216**, 1843–1856 (2019).
19. S. Kumar, V. R. Fonseca, F. Ribeiro, A. P. Basto, A. Água-Doce, M. Monteiro, D. Elessa, R. J. Miragaia, T. Gomes, E. Piaggio, E. Segura, M. Gama-Carvalho, S. A. Teichmann, L. Graca, Developmental bifurcation of human T follicular regulatory cells. *Sci. Immunol.* **6**, eabd8411 (2021).
20. S. Song, P. D. Matthias, The transcriptional regulation of germinal center formation. *Front. Immunol.* **9**, 2026 (2018).
21. D. L. Farber, N. A. Yudanin, N. P. Restifo, Human memory T cells: Generation, compartmentalization and homeostasis. *Nat. Rev. Immunol.* **14**, 24–35 (2014).
22. D. Botta, M. J. Fuller, T. T. Marquez-Lago, H. Bachus, J. E. Bradley, A. S. Weinmann, A. J. Zajac, T. D. Randall, F. E. Lund, B. León, A. Ballesteros-Tato, Dynamic regulation of T follicular regulatory cell responses by interleukin 2 during influenza infection. *Nat. Immunol.* **18**, 1249–1260 (2017).
23. P.-G. G. Ritvo, G. Churlaud, V. Quiniou, L. Florez, F. Brimaud, G. Fourcade, E. Mariotti-Ferrandiz, D. Klatzmann, T_{fr} cells lack IL-2Rα but express decoy IL-1R2 and IL-1Ra and suppress the IL-1–dependent activation of T_{fh} cells. *Sci. Immunol.* **2**, eaan0368 (2017).
24. J. B. Wing, Y. Kitagawa, M. Locci, H. Hume, C. Tay, T. Morita, Y. Kidani, K. Matsuda, T. Inoue, T. Kurosaki, S. Crotty, C. Coban, N. Ohkura, S. Sakaguchi, A distinct subpopulation of CD25− T-follicular regulatory cells localizes in the germinal centers. *Proc. Natl. Acad. Sci. U.S.A.* **114**, E6400–E6409 (2017).
25. M.-A. Alyanakian, S. You, D. Damotte, C. Gouarin, A. Esling, C. Garcia, S. Havouis, L. Chatenoud, J.-F. Bach, Diversity of regulatory $CD4^+$ T cells controlling distinct organ-specific autoimmune diseases. *Proc. Natl. Acad. Sci. U.S.A.* **100**, 15806–15811 (2003).
26. M. Ono, J. Shimizu, Y. Miyachi, S. Sakaguchi, Control of autoimmune myocarditis and multiorgan inflammation by glucocorticoid-induced TNF receptor family-related proteinhigh, Foxp3-expressing $CD25^+$ and $CD25^-$ regulatory T cells. *J. Immunol.* **176**, 4748–4756 (2006).
27. V. R. Fonseca, A. Agua-doce, A. R. Maceiras, W. Pierson, F. Ribeiro, V. C. Romão, A. R. Pires, S. L. da Silva, J. E. Fonseca, A. E. Sousa, M. A. Linterman, L. Graca, S. Lopes, J. E. Fonseca, A. E. Sousa, M. A. Linterman, L. Graca, S. L. da Silva, J. E. Fonseca, A. E. Sousa, M. A. Linterman, L. Graca, Human blood T_{fr} cells are indicators of ongoing humoral activity not fully licensed with suppressive function. *Sci. Immunol.* **2**, eaan1487 (2017).
28. P. T. Sage, D. Alvarez, J. Godec, U. H. von Andrian, A. H. Sharpe, Circulating T follicular regulatory and helper cells have memory-like properties. *J. Clin. Invest.* **124**, 5191–5204 (2014).
29. V. Panneton, B. C. Mindt, Y. Bouklouch, A. Bouchard, S. Mohammaei, J. Chang, N. Diamantopoulos, M. Witalis, J. Li, A. Stancescu, J. E. Bradley, T. D. Randall, J. H. Fritz, W.-K. Suh, ICOS costimulation is indispensable for the differentiation of T follicular regulatory cells. *Life Sci. Alliance* **6**, e202201615 (2023).
30. P. T. Sage, L. M. Francisco, C. V. Carman, A. H. Sharpe, The receptor PD-1 controls follicular regulatory T cells in the lymph nodes and blood. *Nat. Immunol.* **14**, 152–161 (2013).
31. K. L. Good-Jacobson, C. G. Szumilas, L. Chen, A. H. Sharpe, M. M. Tomayko, M. J. Shlomchik, PD-1 regulates germinal center B cell survival and the formation and affinity of long-lived plasma cells. *Nat. Immunol.* **11**, 535–542 (2010).
32. C. Stringer, T. Wang, M. Michaelos, M. Pachitariu, Cellpose: A generalist algorithm for cellular segmentation. *Nat. Methods* **18**, 100–106 (2021).

Acknowledgments: We would like to thank the Flow Cytometry, Comparative Pathology and Bioimaging units of Gulbenkian Institute for Molecular Medicine for services and assistance. We thank the Otorhinolaryngology Department of Hospital de Santa Maria, Centro Hospitalar Universitário Lisboa Norte, Lisbon Academic Medical Centre, and Instituto Português do Sangue e da Transplantação for their collaboration. We gratefully thank the participation of all volunteers who donated samples for this study. We sincerely thank J. Malato for valuable assistance with the statistical analysis. **Funding:** This work was supported by the Fundacion la Caixa grant HR22-00741 and the Portuguese Fundação para a Ciência e Tecnologia (FCT) grant 2022.04903.PTDC to L.G. **Author contributions:** Conceptualization: F.R., V.R.F., S.K., and L.G. Methodology: F.R., D.A., A.R.P., J.R., B.F., K.J., and R.C. Software: F.R., J.R., and S.K. Validation: F.R., D.A., and A.R.P. Formal analysis: F.R. and D.A. Investigation: F.R., D.A., A.R.P., J.R., K.J., R.C., and S.K. Resources: F.R., A.R.P., J.R., and B.F. Data curation: F.R. and S.K. Writing—original draft: F.R. and L.G. Writing—review and editing: F.R., D.A., A.R.P., J.R., B.F., K.J., R.C., V.R.F., S.K., and L.G. Visualization: F.R., S.K., and L.G. Supervision: F.R., S.K., and L.G. Project administration: F.R., S.K., and L.G. Funding acquisition: L.G. **Competing interests:** The authors declare that they have no competing interests. **Data and materials availability:** All data needed to evaluate the conclusions in the paper are present in the paper and/or the Supplementary Materials. The data and code for the PCA and the code for microscopy analysis are deposited in Zenodo under the DOIs https://doi.org/10.5281/zenodo.15128189 and https://doi.org/10.5281/zenodo.15130459, respectively.

Submitted 15 October 2024
Accepted 6 June 2025
Published 11 July 2025
10.1126/sciadv.adt8901